



Variable expressivity and novel *PTEN* mutations in Cowden syndrome

Renato Assis Machado, DDS, MDS, PhD,^a Lívia Maris Ribeiro Paranaíba, DDS, MDS, PhD,^b Luciane Martins, BSc, PhD,^c Mário Rodrigues Melo-Filho, DDS, MDS, PhD,^d Thays Teixeira de Souza, DDS, MDS,^e Bruna Lavinias Sayed Picciani, DDS, MDS, PhD,^e Geraldo Oliveira Silva-Junior, DDS, MSc, PhD,^e Marília Heffer Cantisano, DDS, MDS, PhD,^e Breno Amaral Rocha, DDS,^f Fábio Ramoa Pires, DDS, MDS, PhD,^e and Ricardo D. Coletta, DDS, MDS, PhD^a

Cowden syndrome (CS) is a phosphatase and tensin homolog gene (*PTEN*)–associated condition characterized by multiple mucocutaneous hamartomas and an increased risk of malignancies. We reported an isolated case and another of several individuals in one family affected by CS. The isolated case showed typical features, including fibrocystic breast disease, benign thyroid nodules, and multiple papillomatous lesions in the face and oral cavity, and the cause was a novel nonsense mutation—guanine (G) to thymine (T) transition at position 940 (c.940 G>T)—in *PTEN*. In the family, the proband showed erythema nodosum, duodenal ulcer, intestinal polyps, cervical lipoma, renal cysts, and glaucoma, whereas multiple members of her family were found to have intestinal polyps, and a sister had been diagnosed with breast cancer at early age. An intronic mutation—T>G transition at the +32 position of intron 8 (c.1026+32 T>G)—was found in this family, with *in silico* analysis revealing the creation of a new donor splice site. This study confirmed the involvement of *PTEN* in CS and the variable clinical expressivity of disease. (Oral Surg Oral Med Oral Pathol Oral Radiol 2019;127:55–61)

Cowden syndrome (CS; OMIM #158350) is an autosomal dominant condition with a prevalence of approximately 1:200,000.¹ It is characterized by multiple hamartomatous lesions, especially in skin and mucous membranes, and an increased risk of benign and malignant tumors.² Its clinical expression is highly variable.³ A few years after the first report, mutations in the phosphatase and tensin homolog gene (*PTEN*), which is localized in 10q23.2, were associated with CS.⁴ Mutations in *PTEN* have been also described in Bannayan-Riley-Ruvalcaba syndrome, Lhermitte-Duclos disease, and possibly Proteus syndrome.⁵ Although those disorders show distinctive clinical features, they are

grouped together under the spectrum of *PTEN*-hamartoma tumor syndrome.⁶

Currently, it is accepted that most patients with typical features of CS have *PTEN* mutations, and the remainder remains unexplained, suggesting a possible genetic heterogeneity for this disease.^{2,6} Here, we report one isolated case of CS (de novo mutation) and one family with several members affected by CS displaying *PTEN* mutations and variable clinical expressivity. Molecular analysis identified a heterozygous nonsense mutation (c.940 G>T) in exon 8 of *PTEN* in the isolated case; in the family, affected individuals demonstrated a homozygous c.1026+32 T>G in *PTEN*, which is predicted to create a new splicing site.

This work was supported by grants from The State of São Paulo Research Foundation-FAPESP, São Paulo, Brazil (2016/02667-0).

^aDepartment of Oral Diagnosis, School of Dentistry, University of Campinas, Piracicaba, São Paulo, Brazil.

^bDepartment of General Pathology, Federal University of Alfenas, Minas Gerais, Brazil.

^cDepartment of Prosthodontics and Periodontics, Division of Periodontics, School of Dentistry, University of Campinas, Piracicaba, São Paulo, Brazil.

^dStomatology Clinic, Dental School, University of Montes Claros, Montes Claros, Minas Gerais, Brazil.

^eDepartment of Oral Pathology, School of Dentistry, State University of Rio de Janeiro, Rio de Janeiro, Brazil.

^fPost-graduation Program in Dentistry, School of Dentistry, Pontifícia Universidade Católica de Minas Gerais, Belo Horizonte, Minas Gerais, Brazil.

Received for publication May 15, 2018; returned for revision Aug 13, 2018; accepted for publication Aug 26, 2018.

© 2018 Elsevier Inc. All rights reserved.

2212-4403/\$-see front matter

<https://doi.org/10.1016/j.oooo.2018.08.016>

MATERIALS AND METHODS

Written informed consent was obtained in compliance with the tenets of the Declaration of Helsinki—Ethical Principles for Medical Research Involving Human Subjects.

Mutational analysis of candidate gene

Genomic DNA was isolated from the buccal mucosa cells by using a salting-out protocol.⁷ *PTEN* genomic variants were detected by DNA direct sequencing in family members enrolled in the study. *PTEN* was amplified by polymerase chain reaction (PCR) by using primers designed to investigate all exons and splicing junctions (Supplementary Table I). Direct DNA sequencing of PCR products was performed by using the BigDye Terminator v3.1 Cycle Sequencing Kit (Applied Biosystems, Foster City, CA) and migrated

on capillary 3500 Genetic Analyzer (Applied Biosystems, Foster City, CA).

Residue conservation analysis

Multiple-species amino acid sequence alignment of the PTEN protein was performed by using Clustal Omega (European Bioinformatics Institute, EMBL-EBI; <http://www.ebi.ac.uk/Tools/msa/clustalo/>). Sequence logo for PTEN sequences was carried out by using WebLogo analysis.⁸ The following PTEN sequences were used: human (NP_000305.3), monkey (NP_001247894.1), chimpanzee (XP_016774311.1), mouse (NP_032986.1), rat (NP_113794.1), dog (NP_001003192.1), cat (XP_003993913.1), pig (NP_001137168.1), cattle (XP_002698416.1), chicken (XP_015134187.1), frog (NP_001116943.1), and zebrafish (NP_001001822).

PTEN structure and contact analysis

Three-dimensional (3-D) models for the native and mutant (p.E314*) forms based in the isoform A of PTEN (UniProt: F6 KD01) and in the previously determined wild-type crystal structure 1D5R.1.A,⁹ were built by using the SWISS-MODEL software.¹⁰ The superimposition of the predicted 3-D structure of p.E314* mutant PTEN with wild-type PTEN structure, alignment, visualization, and analysis of the models were made by using the PyMOL software (PyMOL Molecular Graphics System, version 1.7.4, Schrödinger, LLC, New York).

In silico splicing prediction

The intronic mutation found in the *PTEN* gene (c.1026+32 T>G) was analyzed in the context of in silico splicing prediction by means of Alamut[®] Visual version 2.9 (Interactive Biosoftware, Rouen, France), which included 5 prediction algorithms (SpliceSite-Finder-like, MaxEntScan, NNSPLICE, GeneSplicer, and Human Splicing Finder). We focused exclusively on the potential impact of the *PTEN* intronic variant in terms of the disruption of known splice sites or the creation of new potential splice sites.

CLINICAL REPORT

Isolated case

A 34-year-old female was referred with a chief complaint of a 1-year history of oral lesions. During anamnesis, the patient reported fibrocystic breast disease and an intracystic papilloma in the right breast, multiple benign thyroid nodules, gallbladder calculi, pulmonary centrilobular nodules with formation of air cysts, and previously removed epidermoid cysts on her back. Physical examination revealed multiple facial skin papules compatible with trichilemmomas, conjunctival papules, acral keratosis in the palms, and several papules also on the neck and axillae (Figures 1A to 1D). Oral examination revealed the presence of multiple disseminated keratotic

papules on the gingiva, alveolar mucosa, and tongue, with the tongue also presenting fissured areas (Figures 1E and 1F). A hyperplastic growth with a papillary surface was also observed in the gingival area close to the right retromolar zone (Figure 1G). The clinical diagnosis was multiple hamartomas associated with CS. The patient complained that the retromolar lesion and 2 other lesions in the anterior upper gingiva made it difficult for her to perform local oral hygiene (inducing sporadic bleeding episodes), and the 3 lesions were surgically removed under cover of local anesthesia. Histologic analysis revealed the presence of an acanthotic, parakeratinized, stratified squamous epithelium with focal papillary areas, and the subjacent connective tissue was permeated by a chronic inflammatory infiltrate and numerous small blood vessels (Figure 1H). The diagnosis was compatible with fibroepithelial inflammatory hyperplasia. The patient was referred for medical evaluation, and surgical removal of some of the skin papules confirmed the diagnosis of trichilemmomas. The patient remains stable and in clinical follow-up for 60 months. No abnormalities were observed in other family members.

Mutational screening revealed c.940 G>T within exon 8 of *PTEN*, which results in substitution of glutamate (E), at nucleotide position 314, by a stop codon (p.E314*) in the proband (Figure 2A). This substitution was not detected in the proband's parents. Domain and residue conservation analyses showed that the E314 is highly conserved among mammalian and vertebrate species (Figures 2B and 3C), and 3-D structure analysis revealed that the E314 residue is located in the *c*β7-strand structure of the C2 domain and that the mutation causes the loss of 89 amino acids, resulting in loss of the loop and terminal portion of the domain (Figure 3).

Familial cases

A 68-year-old woman (proband) was referred for evaluation of a lump in her tongue; the lump had been increasing in size for the past 2 years. Previous medical history revealed bladder endometriosis, erythema nodosum in the leg, uterine myoma, duodenal ulcer, multiple intestinal polyps, colloid goiter with hyperplastic areas and lymphocytic thyroid, cervical lipoma, cortical renal cysts, and glaucoma. The patient was taking calcium carbonate, levothyroxine, hydrochlorothiazide, and sigmatriol. Her family history revealed 2 paternal siblings (sister and brother) affected by multiple intestinal polyps and 1 sister by breast cancer and intestinal polyps (Supplementary Figure 1). On physical examination of the proband, multiple cutaneous papules were seen on the face and neck (Figures 4A to 4C), and intraoral examination revealed a nodular lesion of soft, elastic consistency and violet coloration, located at the right lingual apex (Figure 4D). In view of extraoral and intraoral clinical



Fig. 1. Images of isolated case of Cowden syndrome (CS). Photographs showing multiple facial (A) and cervical (B) skin papules compatible with trichilemmomas, conjunctival papules (C), and acral keratosis in the palms (D). Multiple, disseminated keratotic papules in the gingiva and alveolar mucosa (E). Fissured tongue showing multiple papules (F); and hyperplastic papillary growth in the right retromolar area (G). Hematoxylin and eosin (H&E)-stained section of the retromolar area showed acanthotic, parakeratinized, stratified squamous epithelium covering connective tissue permeated by an intense inflammatory infiltrate (H) (original magnification $\times 400$).

manifestations, as well as previous medical and family history, the diagnostic hypothesis of CS was considered. The tongue lesion was removed, and the result of the histologic analysis was compatible with intravascular papillary endothelial hyperplasia (Masson's tumor) (Figures 4E and 4F). The patient is currently under medical and dental follow-up, and no signs of recurrence of the tongue lesion have been observed.

Family members of the proband affected by CS demonstrated an intronic *PTEN* mutation (c.1026+32 T>G) (Supplementary Figure 2). Asymptomatic members of this family showed a native sequence. In silico analysis of c.1026+32 T>G mutation revealed the creation a new and viable donor splice site, with high predicted scores in all algorithms (SpliceSiteFinder-like, MaxEntScan, and Human Splicing Finder) (Table I).

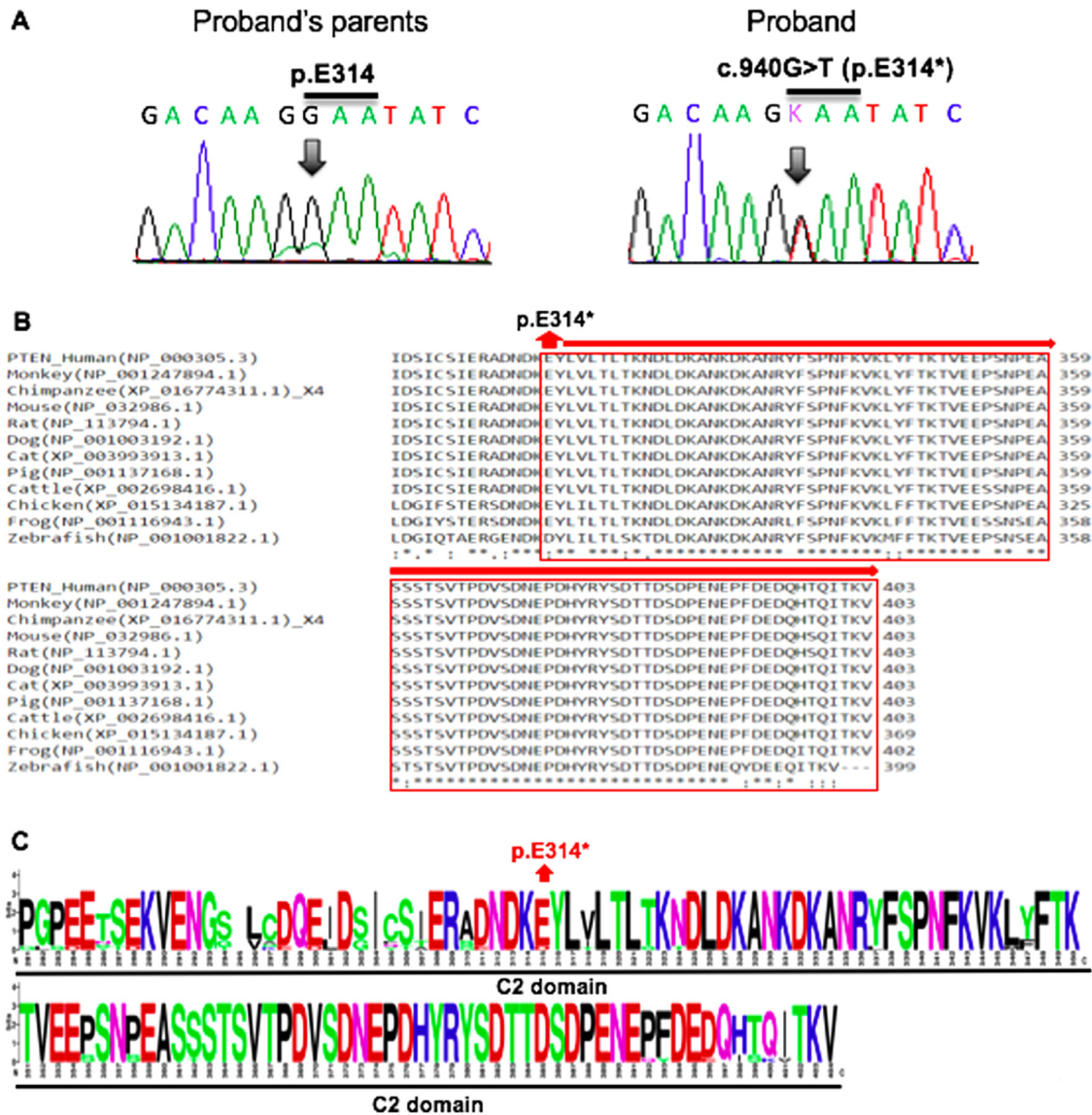


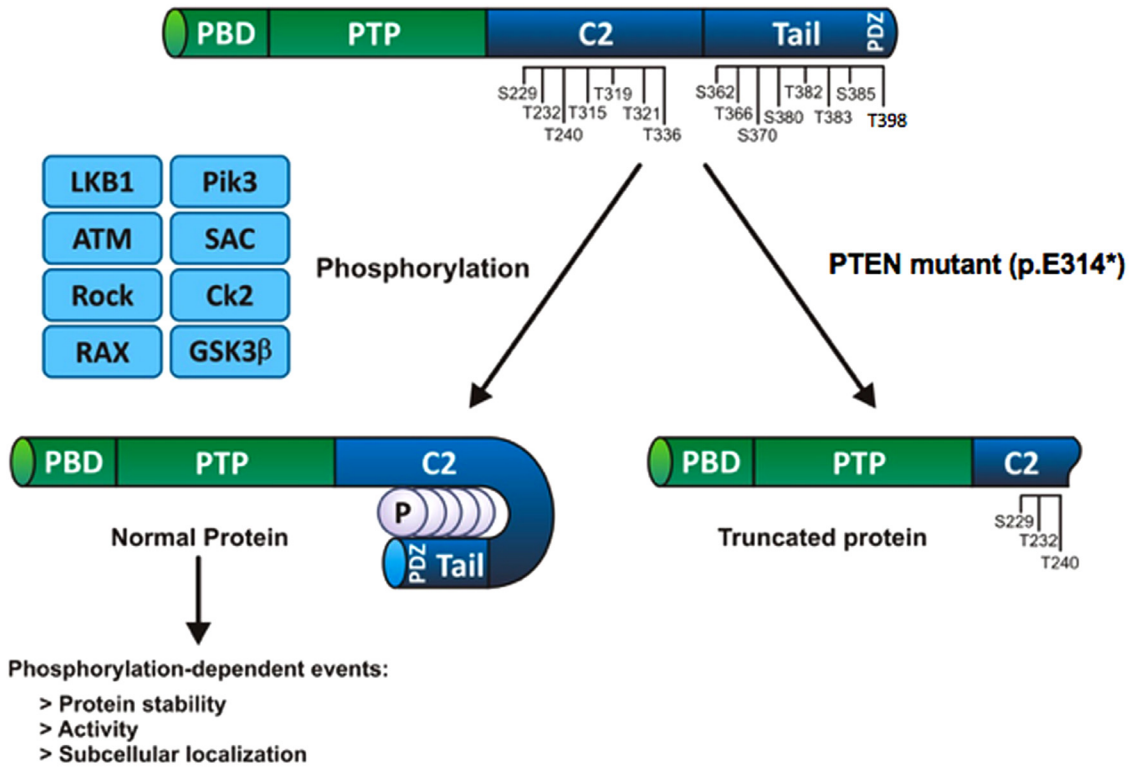
Fig. 2. Identification of missense mutation in *PTEN* gene and residue conservation analysis in the isolated case. (A) Chromatograms of DNA sequencing from the proband showing a de novo heterozygous c.940 G>T, GAA>TAA transversion, which results in a p.Glu314* (E314*) mutation in *PTEN* and a representative normal chromatogram of proband's parents. (B) *PTEN* protein sequences alignment from different organisms, indicating that the E314 residue (indicated by the arrow) is highly conserved in mammalian and vertebrate species. The rectangle indicates the amino acid sequence lost by the c.940 G>T mutation. Multiple-species protein sequences alignment was generated by Clustal Omega tool. (C) Weblogo analysis for *PTEN* C2 domain (281 to 404 aa). The position of E314 native residue, affected by p.E314* mutation, is indicated by a red arrow. The positions of amino acids in the *PTEN* protein sequence are indicated in the horizontal axis, and the height of each symbol reflects its prevalence at the given position.

DISCUSSION

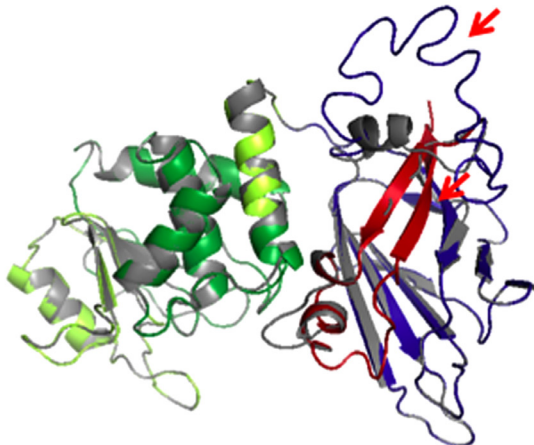
CS is characterized by phenotypic variability, so affected individuals often undergo numerous medical evaluations before a conclusive diagnosis can be made. Although several minimal clinical criteria for definitive diagnosis of CS were proposed,² *PTEN* genetic testing is still required in individuals with typical clinical features. In the current isolated case, the patient

demonstrated typical mucocutaneous lesions, including trichilemmomas, palm keratoses, multiple cutaneous facial papules, and oral mucosal papillomatosis, in association with breast, thyroid, and lung lesions, all of which necessitated *PTEN* genetic analysis. The de novo *PTEN* mutation c.940 G>T in exon 8, which generates a truncated protein lacking 89 amino acids, was identified. In as many as 45% of cases, CS may be

A



B



C



Fig. 3. (A) Schematic representation of the functional domains of PTEN protein which consists of an N-terminal domain (green) and a C-terminal domain (blue). PTEN localization, activity, and stability are controlled by phosphorylation. Phosphorylation of PTEN in the C-terminal tail by kinases decreases membrane association and protein activity but enhances protein stability. Phosphorylation of residues in the C-terminus of PTEN might cause the C-terminal tail to interact with the C2 domain, inducing closed conformation and predominantly cytosolic localization, which inhibit PTEN activity. (B) Superimposed 3-dimensional (3-D) models from native PTEN proteins, showing an N-Terminal protein tyrosine phosphatase (green) and more C-terminal C2 domain (blue) and p.E314* (gray) mutants. The red arrows indicates loss of the loop and the terminal portion of the C2 domain (red). (C) 3-D model from p.E314* mutant.

caused by de novo *PTEN* mutations,¹¹ but it has been suggested that many cases of de novo CS, indeed, result from mosaicism in a parent.¹² In the isolated case presented here, the patient's parents showed no mutations on *PTEN*, eliminating mosaicism as the cause of her disease. Cases without a family history of

CS (de novo CS or mosaicism) make it difficult to arrive at a definitive diagnosis of this condition.

Although lesions in the oral cavity, mainly characterized by oral papillomatosis, are frequently reported in patients with CS, with some authors suggesting that the presence of those features is critical for CS

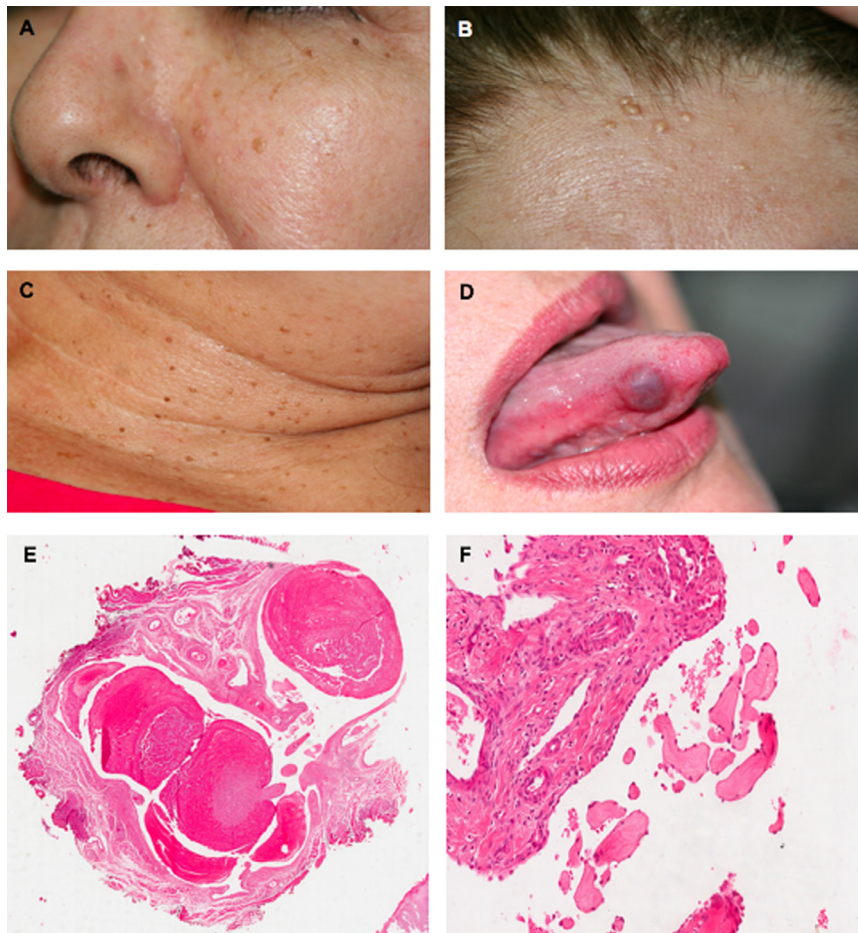


Fig. 4. Images of the proband of the family with multiple individuals with Cowden syndrome (CS). Photograph showing multiple, normochromic, cutaneous papules on the face and neck (A–C). Intraoral photograph showing a nodular lesion of soft, elastic consistency and violet coloration, approximately 2cm in size, and located at the right lingual apex (D). Histopathologic features showing organized thrombus occupying a dilated vessel (E) (original magnification $\times 100$) and papillary projections surrounded by plump endothelial cells with hyaline bundles (F) (original magnification $\times 400$).

diagnosis, in the family case reported here, members of the proband’s family did not show those lesions. Indeed, the diagnosis of CS was only suspected after anamnesis and clinical examination of the proband in association with information regarding various members of family with multiple intestinal polyps and a

sister with breast cancer diagnosed at an early age. Development of cancer in multiple organs is frequent in patients with CS, but the most common cancers include female breast, endometrial, thyroid, colon, and renal cancers.² Genetic analysis of those family members with clinical phenotypes related to CS revealed a substitution in a critical splicing site region at the exon 8–intron 8 junction, creating a new and viable donor splice site, as predicted by different algorithms. Thus, this study reinforces the importance of family medical history for the diagnosis of CS.

Table 1. In silico splice site prediction for intronic mutation in *PTEN* (c.1026+32 T>G)

Algorithms	Normal sequence	c.1026+32 T>G
SpliceSiteFinder-like [0–100]	0	dss 70.3
MaxEntScan [0–16]	0	dss 1.2
NNSPLICE [0–1]	0	0
GeneSplicer [0–15]	0	0
Human Splicing Finder [0–100]	0	dss 80.1

c.1026+32 T>G, T to G transition at position 1026+32 of *PTEN*; dss, donor splice site.

CONCLUSIONS

This study found novel mutations in patients with CS, confirming the variable clinical expressivity of signals. Although both mutations have been described in cancer tissues,^{13,14} germline *PTEN* mutations are rare, and additional phenotypic features are almost always

identified in CS cases. Patients with CS should, therefore, be educated about the need for cancer surveillance.

SUPPLEMENTARY MATERIALS

Supplementary material associated with this article can be found in the online version at <https://doi.org/10.1016/j.oooo.2018.08.016>.

REFERENCES

1. Farooq A, Walker LJ, Bowling J, Audisio RA. Cowden syndrome. *Cancer Treat Rev.* 2010;36:577-583.
2. Gammon A, Jasperson K, Champine M. Genetic basis of Cowden syndrome and its implications for clinical practice and risk management. *Appl Clin Genet.* 2016;9:83-92.
3. Flores IL, Romo SA, Tejeda Nava FJ, et al. Oral presentation of 10 patients with Cowden syndrome. *Oral Surg Oral Med Oral Pathol Oral Radiol.* 2014;117:e301-e310.
4. Liaw D, Marsh DJ, Li J, et al. Germline mutations of the *PTEN* gene in Cowden disease, an inherited breast and thyroid cancer syndrome. *Nat Genet.* 1997;16:64-67.
5. Blumenthal GM, Dennis PA. PTEN hamartoma tumor syndromes. *Eur J Hum Genet.* 2008;16:1289-1300.
6. Pilarski R, Eng C. Will the real Cowden syndrome please stand up (again)? Expanding mutational and clinical spectra of the PTEN hamartoma tumour syndrome. *J Med Genet.* 2004;41:323-326.
7. Aidar M, Line SRP. A simple and cost-effective protocol for DNA isolation from buccal epithelial cells. *Braz Dent J.* 2007;18:148-152.
8. Crooks GE, Hon G, Chandonia JM, Brenner SE. WebLogo: a sequence logo generator. *Genome Res.* 2004;14:1188-1190.
9. Lee JO, Yang H, Georgescu MM, et al. Crystal structure of the PTEN tumor suppressor: implications for its phosphoinositide phosphatase activity and membrane association. *Cell.* 1999;99:323-334.
10. Bordoli L, Kiefer F, Arnold K, et al. Protein structure homology modeling using SWISS-MODEL workspace. *Nat Protoc.* 2009;4:1-13.
11. Mester J, Eng C. Estimate of de novo mutation frequency in probands with PTEN hamartoma tumor syndrome. *Genet Med.* 2012;14:819-822.
12. Gammon A, Jasperson K, Pilarski R, Prior T, Kuwada S. PTEN mosaicism with features of Cowden syndrome. *Clin Genet.* 2013;84:593-595.
13. Cohn DE, Basil JB, Venegoni AR, et al. Absence of PTEN repeat tract mutation in endometrial cancers with microsatellite instability. *Gynecol Oncol.* 2000;79:101-106.
14. Cheng Y, Pang JC, Ng HK, et al. Pilocytic astrocytomas do not show most of the genetic changes commonly seen in diffuse astrocytomas. *Histopathology.* 2000;37:437-444.

Reprint requests:

Renato Assis Machado
Department of Oral Diagnosis School of Dentistry
University of Campinas
Piracicaba, São Paulo, Brazil
renatoassismachado@yahoo.com.br